Enhancement of Linear Compressor Power and Performance Improvement of Pulse Tube Refrigerator

B. Kim, D. Kwon, and S. Jeong

Cryogenic Engineering Laboratory, Department of Mechanical Engineering,
Korea Advanced Institute of Science and Technology (KAIST)
Daejeon 34141, Republic of Korea

ABSTRACT

The performance of a pulse tube refrigerator (PTR) is investigated by increasing the power of the cold linear compressor. In previous research, the cold linear compressor, which operated at liquid nitrogen temperature, was successfully demonstrated and produced sufficient acoustic power for operating a PTR to reach 20 K. Although the PTR using a cold compressor achieved a cooling power of 0.4 W at 20 K, it was found that the regenerator performance was poor because of insufficient acoustic output power from the compressor.

To increase the output power using the same linear motor, a new piston-cylinder assembly was fabricated. The diameter of the piston was enlarged from 27 mm to 33 mm, and the surfaces of the piston and cylinder were coated with polytetrafluoroethylene (PTFE) and nickel, respectively. The linear compressor using the new piston produces about 56 W of acoustic power, which is 43% larger than the previous result. The cooling performance of the PTR was, therefore, improved accordingly with more input power. The PTR with modified compressor achieves a no-load temperature of 17.8 K and a cooling capacity of 1.1 W at 20 K. This paper presents the detailed design issues of incorporating the new cold linear compressor into the PTR.

INTRODUCTION

Regenerative cryocoolers, such as Gifford-McMahon (GM), Stirling, and pulse tube cryocoolers, have been used in many applications.[1,2,3] Especially, the Stirling-type pulse tube refrigerator (SPTR) has demonstrated high reliability, low vibration, and compactness. A SPTR makes use of the oscillation of pressure and mass flow in order to achieve the cooling effect. The oscillation of pressure and mass flow can be produced by various compressors. Among those compressors, the linear compressor is characterized by high efficiency and long-life time.[4,5] The linear motor inside the linear compressor enables driving forces to act along the direction of piston motion, which leads to less friction between the piston and the cylinder wall. Thus, the piston motion, such as stroke and direction, is easily controlled, and a high mechanical efficiency can be achieved with a relatively simple structure. Because of those advantages, a linear compressor is commonly adopted in SPTRs. In the linear compressor, the simple back and forth movement of the piston generates the oscillation of both pressure and mass flow. The governing equation of the piston movement can be expressed as a simple 2nd order differential equation related with the pressure force and

Cryocoolers 21, edited by R.G. Ross, Jr., J.R. Raab and S.D. Miller
© International Cryocooler Conference, Inc., Boulder, CO, 2021

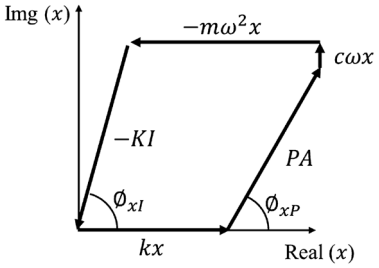

Figure 1. Phase diagram of forces related to motion of the piston: x is piston displacement, k is piston-mount spring stiffness, ω is drive frequency, c is piston damping coefficient, m is mass of piston assembly, P is generated pressure, A is piston area, I is drive current, K is motor force constant, Ø is phase angle.

the driving electromagnetic force. Therefore, the piston movement and the resultant pressure oscillation are correlated to each other. The typical vector diagram of the force related to the piston movement, the pressure force (PA), and the driving force (KI) are shown in Fig. 1. The amplitude ratio and the relative phase between the piston movement and the pressure oscillation are determined by the impedance of the system. When the impedance of the linear compressor and that of the PTR's cold head are mismatched, the linear compressor is unable to produce the oscillation of pressure and mass flow effectively. In previous research, our group developed an SPTR operating with a linear compressor.[6] The target specification of that SPTR was 1 W of cooling power at 20 K. The SPTR succeeded in achieving a no-load temperature below 20 K. The cooling power, however, was less than what was desired. The main cause, we suspected, was the lack of input acoustic power from the linear compressor. The displacement of the piston reached its upper limit before the maximum current was supplied to the linear compressor. This phenomenon happens when the acoustic resistance of the cold head is relatively small.[7] In general, the impedance can be matched by either modifying the cold head to the existing linear compressor, or vice versa.[8] Compared to the former choice, the later choice is challenging, since it requires the capability to manufacture the linear compressor. The linear compressor consists of a housing, the linear motor, and the piston-cylinder assembly. Here, we only changed the piston-cylinder assembly to modify the impedance so that the maximum current is able to be supplied to the linear compressor without exceeding the upper limit of the displacement. The piston-cylinder assembly can be manufactured easily without affecting the design the linear motor. Since the impedance of the cold head remained unchanged, the newly designed piston-cylinder should be well matched to the previous PTR's cold head.

The remainder of the paper describes the impedance matching between the linear compressor and the cold head by redesigning the piston. In addition, experimental results including the demonstration of improved cooling performance of the PTR are presented and discussed.

DESIGN PROCESS

A schematic diagram and photo of the PTR's cold head are shown in Fig. 2. The cold head is of the in-line type and consists of a regenerator, a pulse tube, an inertance tube, and a buffer. The cold head of

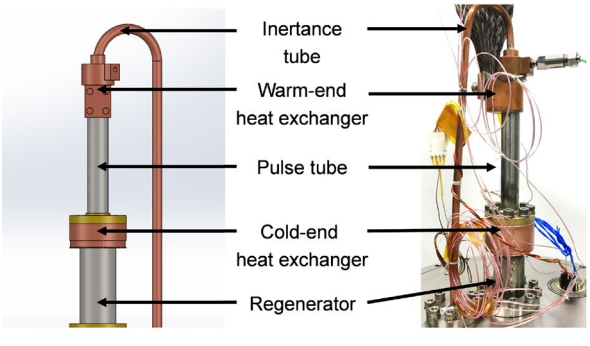

Figure 2. Schematic diagram and photo of the cold head

Table 1. Detailed information of the cold head

Regenerator	22.6 mm (O.D.), 40 mm (L), 0.3 mm (t) 30 mm: #400 stainless steel mesh, porosity 0.65 10 mm: 86 μm-diameter lead powder, porosity 0.35
Pulse tube	12.7 mm (O.D.), 75 mm (L), 0.3 mm (t)
Inertance tube	4.95 mm (I.D), 2.2 m (L) 3.6 mm (I D) 0.24 m (L)
Buffer	500 cc (V)

PTR is installed inside a cryostat and uses a radiation shield to mitigate the heat leak from the ambient; the buffer was installed outside of the cryostat. The detailed specifications of the PTR's cold head are listed in Table 1. The piston and cylinder assembly of the linear compressor need to be manufactured with a clearance seal below 20 μm radial clearance to minimize blowby leakage, and the cylinder must be redesigned when the diameter of the piston changes. Consequently, the size of the piston and the compression volume in the cylinder should be considered simultaneously during the design process. To find the appropriate combination of the size of the piston and the compression volume, the impedance of the cold head without the compression volume is calculated from the measured pressure and the piston movement. A pressure transducer is then installed in the compression space and measures the amplitude and the phase of the oscillating pressure. An accelerometer is mounted on the piston and measures the amplitude and the phase of the acceleration of the piston. Since the piston moves in a sinusoidal way, the velocity or the displacement of the piston can be calculated from its acceleration. More details of the experimental setup can be found in a previous paper.[7] The impedance (Z) of the cold head without compression volume can be calculated from the equations below:

$$Z_{load}{}^{-1} = \boldsymbol{U}A/\boldsymbol{P} = Z_{comp}{}^{-1} + Z_{coldhead}{}^{-1} \tag{1}$$

$$Z_{comp} = -j\gamma P_0/\omega V_0 \tag{2}$$

where $\boldsymbol{P}$ is the measured oscillating pressure, $\boldsymbol{U}$ is the measured piston velocity, A is the area of the piston, V_0 is the compression volume, P_0 is the mean pressure, γ is the specific heat ratio of helium, and ω is the angular frequency. The impedance of the load can be calculated from the measured pressure and the velocity of the piston, and the impedance of cold head is obtained by subtracting the impedance of the compression volume. The equation of the motion of piston is given by Equation (3):

$$\mathrm{j}\omega m\boldsymbol{U} + c\boldsymbol{U} + \left(\frac{k}{\omega j}\right)\boldsymbol{U} = -\boldsymbol{P}A + K\boldsymbol{I} \tag{3}$$

where m is the total mass of the piston assembly, c is the mechanical damping, k is the spring stiffness, K is the motor coefficient, $\boldsymbol{I}$ is the supplied current to the linear motor. The oscillating pressure can be expressed as the velocity of piston and the impedance by applying Equation (1). If the terms related to the mass, damping, and the spring are combined together as a mechanical impedance, Equation (3) can be converted to Equation (4). When the current is supplied, the amplitude and relative phase of the piston's velocity is determined by Equation (4). Based on the velocity of the piston, the amplitude of displacement can be calculated by simply dividing velocity by ω. The calculated amplitude of displacement should not exceed the upper bound of stroke.

$$Z_{total}\boldsymbol{U} = (Z_{mech} + Z_{load}A^2)\boldsymbol{U} = K\boldsymbol{I} \text{ where } Z_{mech} = \mathrm{c} + \mathrm{j}(\omega\mathrm{m} - \mathrm{k}/\omega) \tag{4}$$

In addition to the resultant movement of the piston, the resultant compressor power can be obtained by Equation (5). Some portion of the compressor power in Equation (5) is dissipated by the mechanical damping. The mechanical damping coefficient, however, is negligibly small in our linear compressor. The produced compressor power, thus, is transmitted to the cold head with little mechanical loss. As a result, the acoustic power can be expressed by the supplied current and the impedance of the system as shown in Equation (6). Here, * and Re mean complex conjugate real part of the complex number, respectively.

$$\dot{W}_{compressor} = \frac{1}{2}\mathrm{Re}(K\boldsymbol{I}\boldsymbol{U}^*) = \frac{1}{2}\mathrm{Re}(\mathbf{P}\mathrm{A}\boldsymbol{U}^*) + \frac{1}{2}\mathrm{Re}(c\boldsymbol{U}\boldsymbol{U}^*) \tag{5}$$

$$\dot{W}_{acoustic} = \frac{1}{2}\mathrm{Re}(\mathbf{P}\mathrm{A}\boldsymbol{U}^*) \approx \frac{1}{2}\mathrm{Re}(K\boldsymbol{I}\boldsymbol{U}^*) = \frac{1}{2}\mathrm{Re}\left(\frac{K^2\boldsymbol{I}\boldsymbol{I}^*}{Z^*{}_{total}}\right) \tag{6}$$

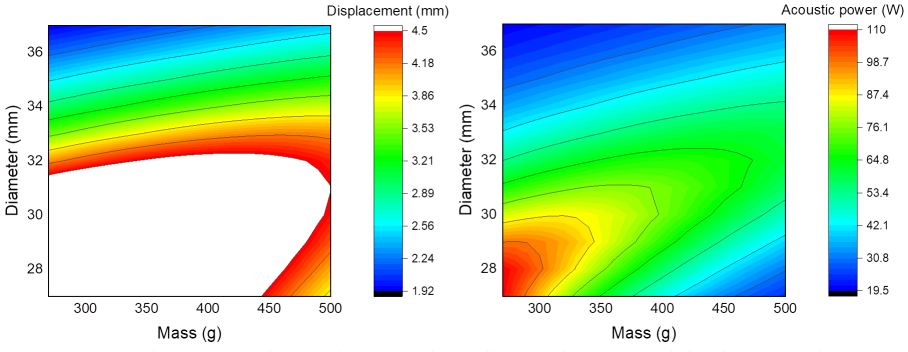

Figure 3. Displacement and acoustic power depending on the mass and the diameter of piston

From Equations (4), (5) and (6), when the amplitude of current is given, the acoustic power is solely affected by the total impedance of the system. When the magnitude of the total impedance is minimum with a pure resistance, the produced acoustic power becomes maximum. The velocity of the piston, however, also becomes maximum, and the displacement may exceed the upper bound of the linear compressor. Therefore, it is important to consider both the upper limit of the displacement of the piston, and the resultant acoustic power. Figure 3 shows the amplitude of the displacement of the piston and the acoustic power depending on the mass and diameter of the piston. The white-colored region represents the infeasible region where the displacement becomes larger than 4.5 mm. Although the stroke limit is about 5 mm, 4.5 mm is selected for safe operation. The combination of the mass and the diameter of the piston should be selected in the feasible region even though the infeasible region allows the largest acoustic power. To select the appropriate combination, the performance of the regenerator was examined using Regen 3.3 regenerator analysis software. According to the numerical analysis, an acoustic power of 50 W to 60 W should be supplied to the cold head. Among the available combinations of mass and diameter for the piston assembly, 410 g and 33 mm were chosen as the mass and the diameter of the new piston assembly. The predicted acoustic power was 60.2 W, which is about 43 % larger compared to the acoustic power with the previous piston assembly design.

EXPERIMENTAL SETUP

Figure 4 shows the manufactured piston-cylinder assembly. The piston and cylinder are made of aluminum, and their surfaces are coated with polytetrafluoroethylene (PTFE) and nickel, respectively. The mass of the piston is 413 g. The radial gap between the piston and the inner surface of the cylinder is about

Figure 4. Photo of piston-cylinder assembly showing radial gap clearance

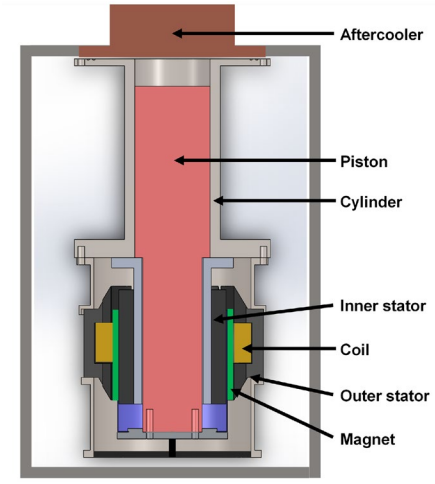

Figure 5. Schematic diagram of the compressor unit

15 micrometers. The magnet is attached to the piston so that the induced magnetic field applies the driving force to the piston. The manufactured piston-cylinder assembly is installed inside the existing linear motor. Thus, the motor coefficient does not change. Figure 5 shows a schematic diagram of the compressor unit. The whole compressor unit including the piston-cylinder assembly, the linear motor, the housing, and the aftercooler is submerged into liquid nitrogen and provides the acoustic power to the cold head. Since the temperature of the compressor unit is maintained at 80 K, there is a chance that the PTFE coating may crack due to the difference in coefficient of thermal expansion of PTFE and aluminum. Fortunately, the PTFE coating adheres on the surface of the piston stably even though the piston is exposed to the repeated heating and cooling between 80 K and room temperature.

The cold head is installed in the cryostat as mentioned before. An AC power source (Chroma programmable AC source 61505) supplies the AC current to the linear compressor. The supplied current is measured by a current probe (Tektronix A622). The oscillating pressure is measured by a piezoelectric pressure sensor (Kistler 601A). The acceleration of the piston is measured by an accelerometer (Kistler 8730AE500M8). E-type thermocouples are installed on the surface of the regenerator, and RTD sensor (Lakeshore Cernox) is mounted on the cold-end heat exchanger. After the refrigerator reaches steady state, a nichrome wire attached on the surface of cold-end heat exchanger is heated, and the amount of the electric power to the nichrome wire is measured at 20 K.

RESULTS AND DISCUSSION

Figure 6 shows the measured current, pressure oscillation and the displacement of the piston when the linear compressor operates. Based on the measured signals, the acoustic power and the compressor

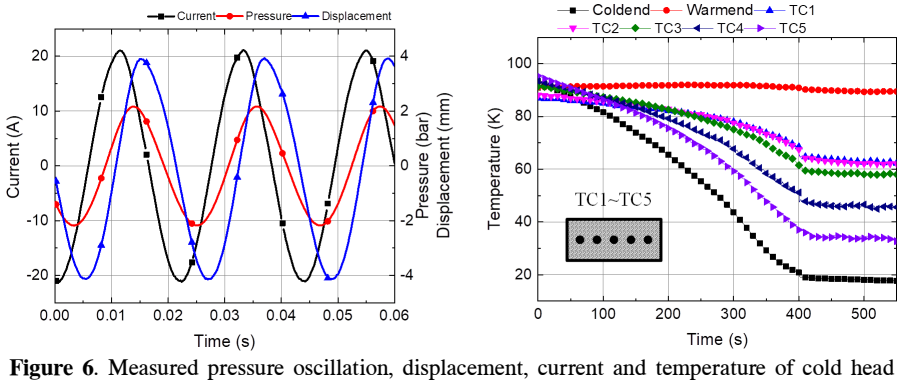

Figure 6. Measured pressure oscillation, displacement, current and temperature of cold head

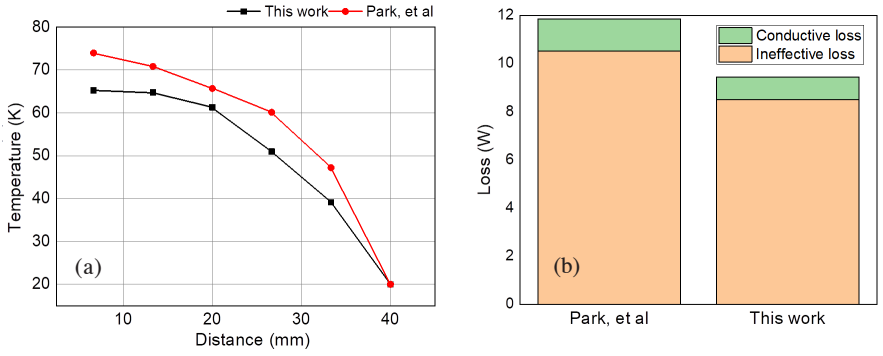

Figure 7. (a) Temperature distribution of the regenerator and (b) the ineffective and conductive losses

power are calculated using Equations (5) and (6). The acoustic power is 56.4 W and the compressor power is 56.5 W, which implies the mechanical loss is negligible. Compared to the expected acoustic power, 60.2 W, the error between the experiment and the calculation is 6.2%. The acoustic power produced by the previous piston was 39.4 W. Thus, the increasing ratio of power is about 43.1%. The cooling capacity of the PTR increased from 0.4 W to 1.1 W at 20 K, and the no-load temperature decreased from 18.7 K to 17.8 K. The relative Carnot COP based on the acoustic power to the cooling power increased from 2.4% to 5.8%.

Figure 7a shows the temperature distribution of the regenerator's surface. The zero distance means the hot end of the regenerator, and the 40 mm distance means the cold end of the regenerator. The temperature distribution with the newly designed piston shows a less steep temperature gradient at the cold side of the regenerator than with the previous piston. The gradient of the temperature becomes steeper at the location of about 30 mm. Since lead powder is packed in the 30 mm to 40 mm section of the regenerator, and the thermal conductivity of the lead is much higher than that of stainless steel, a steeper temperature gradient results in a larger conductive loss. Furthermore, the ineffective loss, which is caused by insufficient heat transfer between the working fluid and the regenerator matrix, may become larger due to the higher inlet temperature of the working fluid. The ineffective and conductive losses with two temperature profiles are compared. The oscillating mass flow rate and the pressure are assumed to be the same in both cases so that the effect of a steeper temperature gradient appears.

Figure 7b shows the conductive loss and the ineffective loss when the temperature profile is assumed the same as the previous and current experimental. Both losses increase when the temperature distribution is steeper at the cold side, which is consistent with the experimental results.

CONCLUSION

To improve the cooling performance of the PTR, the diameter of the piston in the linear compressor was increased. Based on the measured impedance of the PTR's cold head, the expected displacement and the acoustic power were calculated from the mass and the diameter of the piston. Among the feasible combinations of the mass and diameter that do not exceed the displacement limit, a mass of 410 g and a diameter of 33 mm were chosen as the new design specification for the piston. Since the previous piston diameter was 27 mm, the piston and cylinder were manufactured together with the new diameter of 33mm. Both piston and cylinder are made of aluminum. The manufactured piston weighs 413 g, which is 153 g heavier than the previous one, and its surface is coated by PTFE.

The produced acoustic power with the newly designed piston is about 56 W, which is about 43.1% larger than that with the previous piston, and shows good agreement with the calculation results. The cooling performance of the PTR is also improved accordingly with the larger acoustic power from the linear compressor without changing the linear motor. The cooling capacity increased from 0.4 W to 1.1 W at 20 K, and the no-load temperature decreased from 18.7 K to 17.8 K. The relative Carnot efficiency of the PTR also increased from 2.4% to 5.8%.

ACKNOWLEDGMENT

This research was supported by Basic Science Research Program through the National Research Foundation of Korea (NRF-2017R1A2B3003152) funded by the Ministry of Science, ICT & Future Planning (MSIP).

REFERENCES

1. Laskaris, E. T., et al. "A cryogen-free open superconducting magnet for interventional MRI applications," *IEEE transactions on applied superconductivity* 5.2 (1995), pp. 163-168.
2. Duval, J. M., et al. "7K-15K Pulse tube coolers for space," *Cryocoolers 17*, ICC Press, Boulder, CO (2012), pp. 17-23.
3. Otuska, K., et al. "Improvement of micro-vibration of a two stage Stirling cryocooler," *Cryogenics* (2020): 103133.
4. Radebaugh, R. "Advances in cryocoolers," *Proceedings of the Sixteenth International Cryogenic Engineering Conference/International Cryogenic Materials Conference.* Elsevier Science, (1997), pp. 33-44.
5. Liang, K. "A review of linear compressors for refrigeration," *International Journal of Refrigeration,* vol. 84, (2017), pp. 253-273.
6. Park, J., Kwon, S., and Cha, J. "Development and experimental investigation of Stirling-type pulse tube refrigerator (PTR) below 20 K; cold compressor and colder expander," *International Journal of Refrigeration*, vol. 75, (2017), pp. 64-76.
7. Wang, L. Y., et al., "Electric-Mechanical-Acoustic Coupling Characteristics for Pulse Tube Cryocoolers," *Cryocoolers 19*, ICC Press, Boulder, CO (2016), pp. 193-200.
8. Dai, W., et al. "Impedance match for Stirling type cryocooler," *Cryogenics,* vol. 51, no. 4 (2011), pp. 168-172.